ACS Catalysis

Research Article

pubs.acs.org/acscatalysis

Charge-Enhanced Dry Impregnation: A Simple Way to Improve the Preparation of Supported Metal Catalysts

Xiaoru Zhu,[†] Hye-ran Cho,[‡] Malini Pasupong,[†] and John R. Regalbuto*[,‡]

[†]Department of Chemical Engineering (m/c 110), University of Illinois at Chicago, 810 S Clinton Street, Chicago, Illinois 60607, United States

[‡]Department of Chemical Engineering, University of South Carolina, 301 Main Street, Columbia, South Carolina 29208, United States

Supporting Information

ABSTRACT: A simple variation in the method of incipient wetness can dramatically improve metal dispersion in supported metal catalysts. This very common method, also known as dry impregnation or pore filling, often suffers from the absence of metal precursor-support interaction during metal deposition, which usually leads to extensive sintering and poor distribution of the metal phase after pretreatment. In past work, our group has demonstrated the synthesis of ultrasmall nanoparticles in tight size distributions by inducing strong electrostatic interactions between the dissolved metal precursor and support. We have normally employed "wet impregnation" involving thin solution-support slurries, but now show that electrostatic interactions can be induced at incipient wetness. This is done by acidifying or basifying the impregnating solution to the (surprisingly) great extent needed to charge up the surface. With this simple variation we have demonstrated vast improvements in Pt dispersion over carbon, silica, and alumina supports, as characterized by X-ray diffraction (XRD), Z-contrast imaging, and chemisorption. We present calculations from our Revised Physical Adsorption Model which can be used to anticipate the initial pH needed to sufficiently charge a particular surface, such that this approach may be extended to many other metals and supports.

KEYWORDS: *catalyst preparation, dry impregnation, electrostatic adsorption, metal dispersion, point of zero charge, platinum*

INTRODUCTION

Dry impregnation (also called pore filling or incipient wetness) is the simplest, least expensive, and most prevalent way to prepare supported metal catalysts. In this method a desired amount of metal precursor, typically a coordination complex such as platinum hexachloride (PHC, $[PtCl_6]^{2-}$) or platinum tetraammine (PTA, $[(NH_3)_4Pt]^{2-}$), is dissolved in water and the solution is added to an oxide or carbon support in the amount just sufficient to fill the pore volume of the support. The thick slurry/paste is dried and then heated in oxidizing and/or reducing gases to remove the ligands of the precursor and to reduce the metal to its active elemental state. This method requires no filtration, eliminates wasted metal, and yields a precise metal loading.

In dry impregnations no provision is made for the metal precursor complexes to interact with the support surface, and without such interaction, metal complexes agglomerate into large particles either before or during reduction. The most common catalysis metric of metal utilization is dispersion: the fraction of metal atoms appearing at the surfaces of metal crystallites (and available as catalytically active sites), divided by the total number of atoms. Metal nanoparticles one nanometer in diameter have a dispersion of approximately 100%; high dispersion is very often the goal of synthesis. Unlike supported metal oxides, which can be easily dispersed on oxide supports by thermal spreading from mixtures of bulk oxide powders,[1−4] obtaining high dispersion of supported metals requires high dispersion of metal precursors.

Precursor-support interactions in many common catalyst preparations can be envisioned in light of the electrostatic adsorption mechanism[5−9] depicted in Figure 1. Oxide and carbon surfaces terminate in functional groups such as hydroxyls and

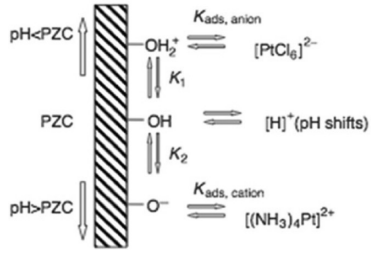

Figure 1. Electrostatic adsorption mechanism.

Received: December 20, 2012
Revised: February 18, 2013
Published: February 20, 2013

carboxylic acids which can protonate or deprotonate as a function of solution pH. At these conditions the surface can electrostatically adsorb precursors of opposite charge; anions adsorb over a protonated surface below the point of zero charge (PZC, the pH at which the surface is neutrally charged), and cations over a deprotonated surface above the PZC.

While it is easy to understand electrostatic adsorption as a function of pH in Figure 1, appreciating the extent of proton transfer in dry impregnation is much less intuitive. Consider, for example, impregnating a typical alumina with a surface area 200 $m^2\ g^{-1}$, pore volume 1.0 $cm^3\ g^{-1}$ and a hydroxyl density of 8 OH nm^{-2}, with a pH 3 solution. This is over five pH units below alumina's PZC of about 8.5; it may be assumed that the low pH solution will protonate the surface and enable adsorption of anions per Figure 1. The number of protons in 1.0 mL (1×10^{-3} L) of pH 3 (10^{-3} molar) solution, equal to the pore volume of the support, is 1×10^{-6} moles. The number of hydroxyl groups on the surface of one gram of alumina support is 1 g $\times$ 200 $m^2\ g^{-1} \times 10^{18}$ $nm^2\ m^{-2} \times 8$ OH(nm^{-2}) $\times$ 1 mol $(6.02 \times 10^{23}$ OH$)^{-1} = 2660 \times 10^{-6}$ moles. With only 1/2660 hydroxyl groups protonated, the surface will be negligibly charged. Enough acid in 1.0 mL of solution to protonate all the surface OH groups would require a concentration of 2.67 mol H/L, or an initial pH of −0.41.

The strong buffering capacity of oxide surfaces at incipient wetness has been pointed out;[10] at this condition the final pH of impregnating solution is almost always at the PZC of the surface and no electrostatic metal precursor-support interaction occurs unless the impregnating solution is made extremely acidic or basic.

Electrostatic adsorption has been demonstrated for the synthesis of ultrasmall (1−2 nm) noble and base metal nanoparticles over a variety of oxide and carbon supports at loadings up to 30 wt %,[11−15] but this approach has employed thin slurries of a powdered support in a large excess of impregnating solution. In this paper we demonstrate that this method can be applied to thick slurries at incipient wetness: electrostatic adsorption will occur by acidifying or basifying the impregnating solution sufficiently to charge the surface. This minor yet critical change in the often-used dry impregnation procedure can vastly improve the metal dispersion for many typical catalyst systems. We further show how this procedure can be extended to many more materials.

EXPERIMENTAL DETAILS

Oxidized carbon (Darco G-60, BET area: 617 m^2/g) and SiO_2 (BET area: 330 m^2/g) were used as low PZC supports with which platinum tetraammine ($[Pt(NH_3)_4]Cl_2$, 99.9%) was used as the precursor. Sodium tetrachloroplatinate(II) ($Na_2PtCl_4\ nH_2O$, 99.9%) from Aldrich were used as the platinum precursor on the high PZC support, a gamma-alumina (BET area: 274 m^2/g) support.

The water accessible pore volume was measured with one gram of oxide and deionized water (pH of 5.6). pH measurements at incipient wetness were made with a spear tip combination pH probe.

DI samples were prepared by adding metal precursor solution for 2 wt % Pt loading. The pastes were dried at room temperature in air and then reduced in hydrogen for 1 h at 200 °C. The same process was used to prepare CEDI samples, with the exception that optimal initial pH values were used (as described later).

Powder X-ray diffraction (XRD) analysis was performed using a Siemens D5000 diffractometer with Cu Kα radiation (λ = 1.5406 Å) operated at 30 kV and 40 mA, operating in Bragg−Brentano geometry. Scans were made in the 10°−90° 2θ range, with step size of 0.02°, and 2 s exposure at each step. Z-contrast STEM imaging for particle size determination in the materials was conducted with a JEOL JEM-2010F FasTEM with a probe size of 0.14−0.2 nm. The catalyst samples were sonicated in isopropanol for 15 min, and the slurry was deposited onto a carbon-coated copper grid (200 mesh, Cu PK/100), supplied by SPI, U.S.A. The applied voltage was 200 kV and extracting voltage of 4500 V. Approximately 500 particles were counted for size distribution. Carbon monoxide chemisorption was used to determine the accessible Pt surface using a Micromeritics ASAP 2020 instrument. The samples were first dried at 110 °C in a He flow for 30 min and subsequently reduced in a 50% H_2/He flow at 350 °C for 2 h (ramp = 10 °C/min).

RESULTS AND DISCUSSION

The amount of acid or base needed to sufficiently charge a surface at incipient wetness, and the effect of the high concentrations of acid and base on metal precursor uptake,

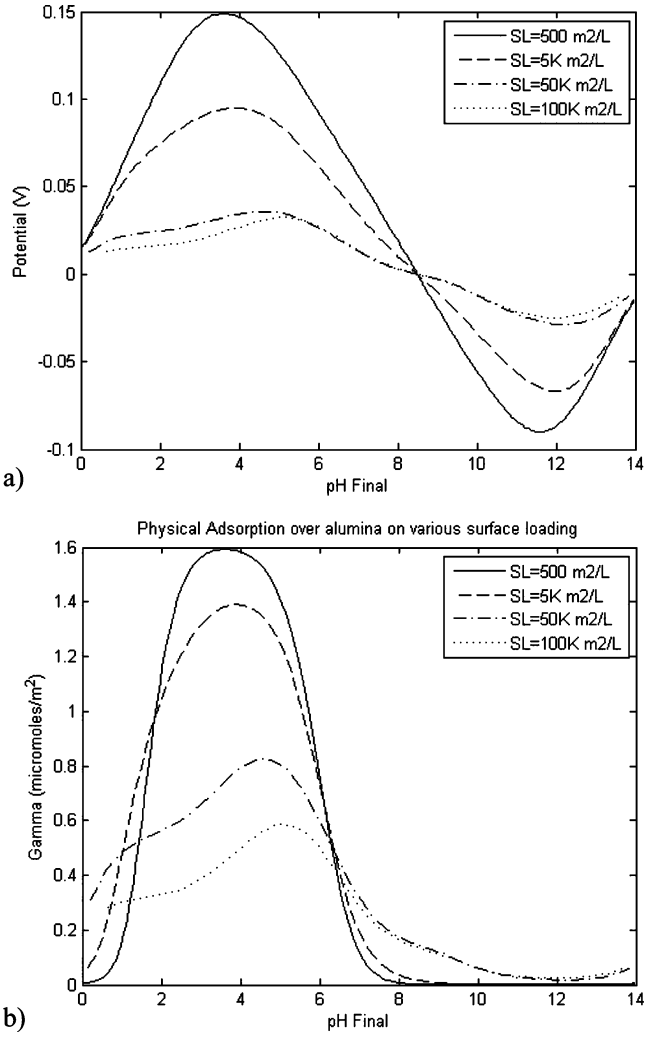

Figure 2. Simulation of SEA at high surface loadings; (a) alumina surface potential, (b) PHC adsorption (PZC 8.5, pk = 5 and Ns = 8 OH/nm^2, SL= 500 m^2/L, PHC initial concentration = 200 ppm).[16]

dx.doi.org/10.1021/cs3008347 | ACS Catal. 2013, 3, 625−630

Table 1. Properties of Supports

supports	BET surface area (m2/g)	pore volume (mL/g)	PZC	optimal pH (final pH)
carbon	617	1.46	1.5	11
SiO_2	330	0.55	3.9	11
Al_2O_3	274	1.85	8.3	3

can be estimated with the revised physical adsorption (RPA) model.[9,16] The model equations and parameters are provided in Supporting Information.

The simulation for PHC adsorption over alumina is given in Figures 2a (potential) and 2b (uptake) at various values of a parameter we call "surface loading," with units $m^2\ L^{-1}$. For any surface loading, the surface potential and metal uptake are zero at the PZC of 8.5. As the pH decreases, uptake initially increases as the surface potential rises, but at the pH extreme, high ionic strength drastically diminishes the adsorption equilibrium constant because of the electric screening.[7−9] Thus metal uptake is a volcano-shaped curve and there exists an optimal pH at which adsorption is strongest.

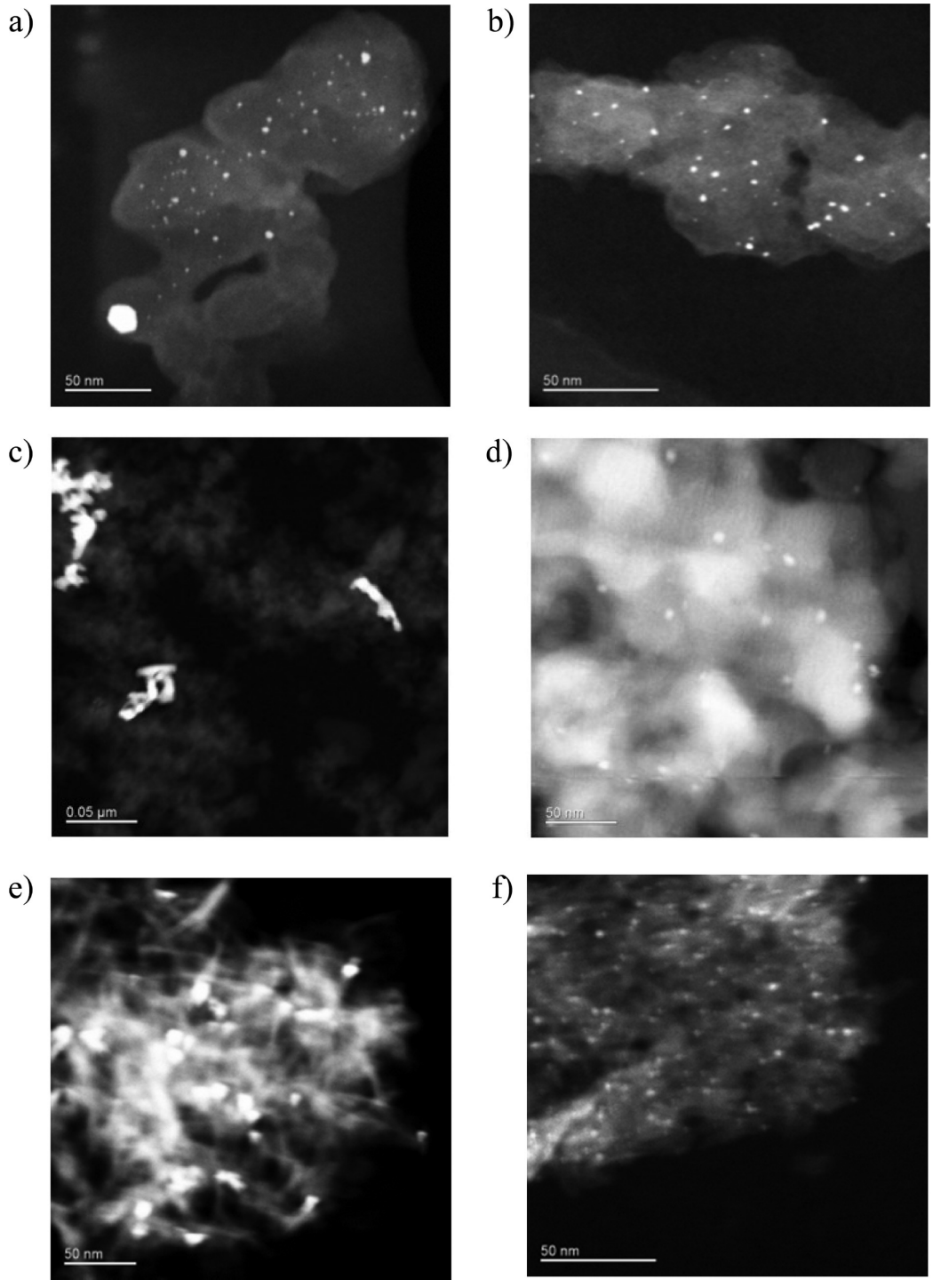

Figure 3. STEM image of Pt catalysts after reduced at 200 °C. (a) Pt/C DI, (b) Pt/C CEDI, (c) Pt/SiO_2 DI, (d) Pt/SiO_2 CEDI, (e) Pt/Al_2O_3 DI, (f) Pt/Al_2O_3 CEDI.

dx.doi.org/10.1021/cs3008347 | ACS Catal. 2013, 3, 625−630

Table 2. Final pH, Particle Size, and Dispersion Analysis for DI and CEDI Samples

	Pt/C DI	Pt/C CEDI	Pt/Al_2O_3 DI	Pt/Al_2O_3 CEDI	Pt/SiO_2 DI	Pt/SiO_2 CEDI
pH_{final}	(1.5)	11.0	(8.3)	3.0	(3.9)	11.0
XRD[a]	14.1	<3	~8	<3	7.9	<3
STEM[a]	10 ± 0.1	1.8 ± 0.1	11 ± 0.1	2.9 ± 0.1	7.5 ± 0.1	1.5 ± 0.1
STEM[b]	10%	56%	9%	34%	13%	67%
CO Chem.[c]	2%	21%	32%	56%	7.6%	71%

[a]Reduced at 200 °C, particle size (nm). [b]Dispersion based on STEM analysis. [c]Reduced at 350 °C, dispersion based on CO chemisorption.

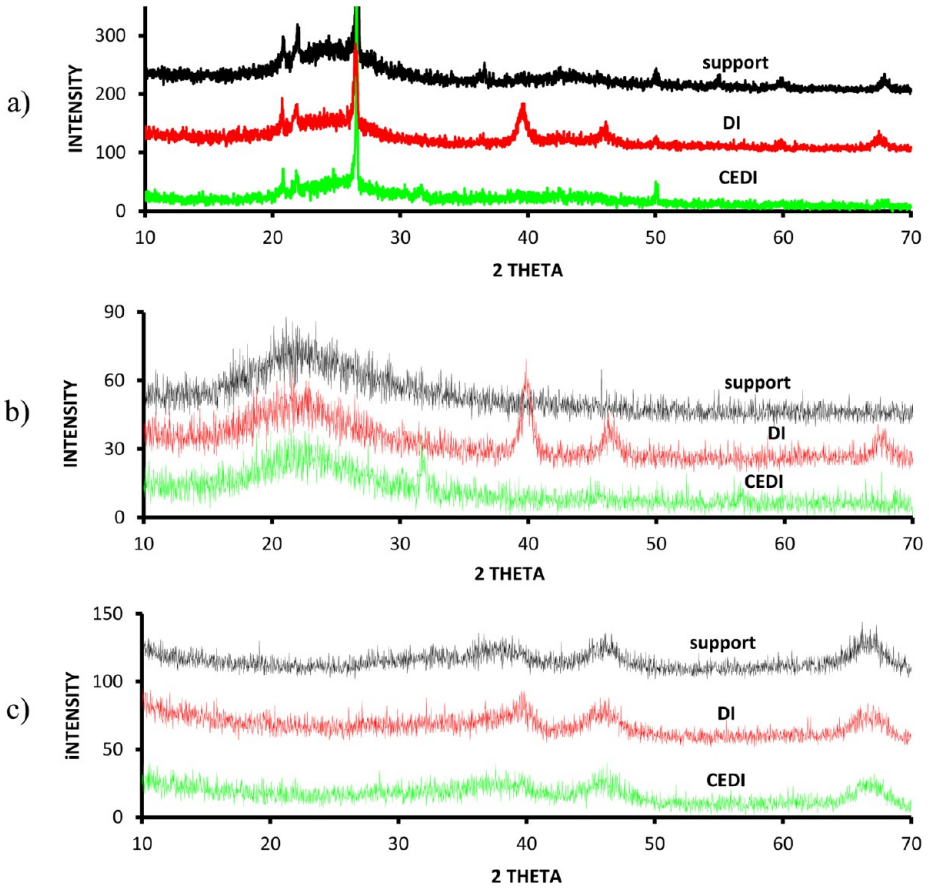

Figure 4. XRD pattern of (a) Pt/C, (b) Pt/SiO_2, and (c) Pt/Al_2O_3, which prepared by DI and CEDI reduced at 200 °C.

Now we consider the effect of surface loading. Thin slurries and correspondingly low surface loadings are convenient for laboratory studies, as low loadings minimize the pH shifts from buffering and make it easy to sample the liquid phase for pH and metal concentration. Most of our studies of "strong electrostatic adsorption" (SEA)[11−15] have employed surface loadings of 500−1000 $m^2\ L^{-1}$.

There is no reason why SEA cannot be employed at higher surface loadings; incipient wetness represents the highest obtainable surface loading for a particular solid. In Figure 2 it is seen that surface potential and metal uptake decrease as surface loading is increased. This decrease is again the result of high ionic strength caused by the balancing electrolytes from the higher concentrations of metal and acid or base. Nonetheless, the simulation predicts a final pH at which electrostatic adsorption is strongest at high surface loading. With enough acid or base (and these amounts are surprisingly large) the final pH can be directed to this optimal value. The correct initial pH to achieve the desired final pH can be estimated from the model, and will be described in detail later. We call this method "charge-enhanced dry impregnation" (CEDI).

Demonstration of Improved Metal Dispersion with CEDI. We have demonstrated CEDI for improving metal dispersion with three catalyst supports and two metal complexes. Table 1 gives the properties of these materials. For the oxidized carbon and silica surfaces that have low PZC, cationic platinum tetraammine was chosen as the metal precursor, and for alumina, which has a high PZC, the anionic platinum tetrachloride complex was used.

STEM analysis was performed on the 2 wt % Pt catalysts after impregnation, drying, and reduction at 200 °C for 1 h at a ramp rate of 5 °C min^{-1}.

Figure 3 shows representative Z contrast STEM images for syntheses by DI and CEDI, and particle sizes with standard deviations are given in Table 2. The average size of nanoparticles prepared by CEDI are 1.8 nm for carbon, 1.5 for silica, and 2.9 for alumina, and are much smaller particles than those prepared by DI, 10, 7.5, and 11 nm, respectively.

dx.doi.org/10.1021/cs3008347 | ACS Catal. 2013, 3, 625−630

Particle size was also characterized by powder XRD; these results are shown in Figures 4a, b, and c for carbon, silica and alumina, respectively. The upper pattern of each set is the pure support. Peaks at 21, 22.5, and 27° 2θ in Figure 4a can be assigned to graphite. After reduction, the Pt on carbon by DI clearly shows fcc Pt with peaks at 39.7° 2θ (111), 46.2° (200), and 67.4° (220). For the CEDI sample, the small peak at 33° 2θ suggests the presence of PtO_2 (from the (200) plane[17]). It is known that the smallest Pt nanoparticles spontaneously oxidize.[18]

The absence of significant Pt peak intensity results from small average particle size. In Figure 4b, on silica the DI sample again clearly exhibits metallic Pt, and again in the CEDI sample only PtO_2 peaks of low intensity are seen. In Figure 4c, fcc Pt peaks overlap the Al_2O_3 support peaks but the Pt(111) peak at 39.7° 2θ for the DI sample is still noticeable, while no Pt peaks are observed for the CEDI sample. Pt particle sizes estimated from the Scherrer equation are given in Table 2 for comparison with the STEM results; the XRD value for the Pt/Al_2O_3 sample is especially rough given the poor signal/noise ratio.

Results of CO chemisorption are also included in Table 2. A reduction of 350 °C was employed so that for the alumina sample all residual chloride would be removed. The CEDI samples for each support exhibited higher CO uptake compared to the DI samples, although the agreement between chemisorption-estimated particle sizes (size in nm = 1/dispersion) is only semiquantitative compared to the XRD and STEM values. The latter two sets of particle sizes are in reasonable agreement.

Extension of CEDI to Other Systems. The key to obtaining maximum metal dispersion with a dry impregnation synthesis procedure is to anticipate the initial pH needed for the impregnating solution. By sufficiently acidifying or basifying the solutions, for a high PZC or low PZC support, respectively, electrostatic adsorption can be achieved.

A potential concern when working with highly acidic or basic solutions is the dissolution of the support at pH extremes. It should be noted, however, that pH equilibration is relatively rapid, typically on the order of minutes, and the support surface will quickly buffer the pH up or down to levels at which the charge is high enough for strong electrostatic adsorption, but moderate enough so that negligible dissolution occurs. In practice, the dropwise or sprayed application of the solution with reasonable mixing of the support should prevent significant support dissolution.

Electrostatic adsorption has been shown to occur over a wide variety of oxides and carbon support materials.[20,21] In many cases, it is the sole adsorption mechanism, or it can occur in conjunction with other mechanism such as ion exchange and deposition-precipitation.[22] To extend CEDI to the many other materials which exhibit electrostatic adsorption, we can employ the RPA model to anticipate the correct initial pH necessary to attain the desired final pH for a particular support material. What needs to be known are the support PZC, which is easily found with pH shift measurements,[10,19] the BET surface area, and the water-accessible pore volume found with a quick water titration. The latter two properties determine the surface loading at dry impregnation, where

$$\mathrm{SL}(\mathrm{m}^2/\mathrm{L}) = [\text{BET surface area } (\mathrm{m}^2/\mathrm{g})]/[\text{pore volume } (\mathrm{L}/\mathrm{g})]$$

Once the PZC and surface loading of the impregnation system are known, the RPA model, which predicts both pH shifts and metal uptake, can be consulted for the proper selection of initial pH. An illustration is given below. The desired final pH can be chosen first with reference to the uptake-pH plot, as illustrated in Figure 5b. For a PZC 2 support, the desired final

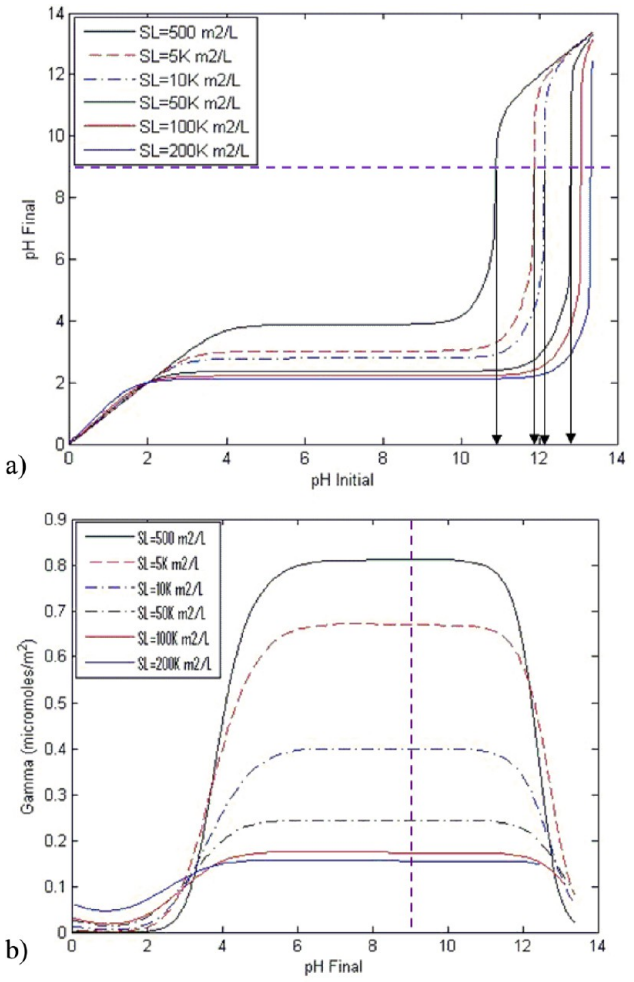

Figure 5. Estimating initial pH for a PZC 2 material, (a) pH shift and (b) uptake-pH calculations.

pH would be 9. (The final pH for this material could actually be in a wider range, as seen in the wide uptake plateau typical of a very low PZC material.) Second, knowing the surface loading which corresponds to dry impregnation, the plot of the pH shift for that material (Figure 5a) is consulted, and the initial pH which corresponds to the desired final pH at the known surface loading is selected. For example, a 100 m^2/g acidic niobium oxide (PZC = 2) with a pore volume of 2 mL/g gives a surface loading of 50,000 m^2/L.

From Figure 5a it is seen that a surface loading of 50,000 m^2/L will require an initial pH of about 12.8 (on the *x*-axis) to arrive at a desired final pH of 9 (*y*-axis). In the Supporting Information we provide large, gridded versions of Figure 5 for other PZC materials.

The accuracy of the pH shift prediction is a logarithmic function of the assumed hydroxyl density, and is thus only weakly dependent on this value. A typical value of 5 OH/nm^2 was used to generate the plots of Figure 5 and the Supporting Information figures and should be sufficient in most cases for a reasonably accurate prediction of the pH shift. In some cases such as unoxidized carbon supports, which have an order of magnitude lower density of surface function groups at low pH

dx.doi.org/10.1021/cs3008347 | ACS Catal. 2013, 3, 625−630

than corresponding oxide surfaces,[15] the pH prediction may be off by one pH unit or so. In any case, the final pH of the dry impregnation paste can be measured with a semisolid pH electrode, of the type used to measure pH in semisolids such as soil and food. Between Figure 5 (and similar figures for other PZC supports in the Supporting Information) for guidance and a few experimental measurements as confirmation, the initial impregnation pH can be quickly determined.

In the Supporting Information are presented large plots of pH shifts and metal uptakes for a range of PZC materials from 2 to 12 (Supporting Information, Figures S1 a–f). Over the low PZC materials (2, 4, and 6 in Supporting Information, Figures S1 a, b, and c), representative of niobia, silica, and anatase titania, a cationic complex such as PTA, $[(NH_3)_4Pt]^{2+}$, would be chosen as precursor. Over high PZC supports (PZCs 8, 10, and 12 are representative of alumina, carbon black, and magnesia, Supporting Information, Figures S1 d, e, and f), an anion such as PHC, $[PtCl_6]^{2-}$, should be chosen.

In this way, charged enhanced dry impregnation can be simply applied to many metals and carbon and oxide supports to optimize metal dispersion in laboratory scale as well as industrial preparations.

■ ASSOCIATED CONTENT

Supporting Information

pH shifts and metal uptakes for a range of PZC materials from 2 to 12 (Figures S1 a–f) from the Revised Physical Adsorption (RPA) model. This material is available free of charge via the Internet at http://pubs.acs.org.

■ AUTHOR INFORMATION

Corresponding Author

*E-mail: regalbuj@cec.sc.edu.

Notes

The authors declare no competing financial interest.

■ ACKNOWLEDGMENTS

Funding for this work is from NSF CBET 0626505.

■ REFERENCES

(1) Haber, J. *Pure Appl. Chem.* **1984**, *56*, 1663–1676.
(2) Stampfl, S. R.; Chen, Y.; J.A. Dumesic, J. A.; Niu, C. M.; Hill, C. G. *J. Catal.* **1987**, *105*, 445–454.
(3) Xie, Y. C.; Tang, Y. Q. *Adv. Catal.* **1990**, *31*, 1–43.
(4) Braun, S.; Appel, L. G.; Camorim, V. L.; Schmal, M. *J. Phys. Chem. B* **2000**, *104*, 6584–6590.
(5) Brunelle, J. P. *Pure Appl. Chem.* **1978**, *50*, 211–232.
(6) Heise, M. S.; Schwarz, J. A. *J. Colloid Interface Sci.* **1985**, *107*, 237–243.
(7) Heise, M. S.; Schwarz, J. A. *J. Colloid Interface Sci.* **1986**, *113*, 55–61.
(8) Heise, M. S.; Schwarz, J. A. *J. Colloid Interface Sci.* **1988**, *123*, 51–58.
(9) Hao, X.; Spieker, W. A.; Regalbuto, J. R. *J. Colloid Interface Sci.* **2003**, *267*, 259–264.
(10) J. Park, J.; Regalbuto, J. R. *J. Colloid Interface Sci.* **1995**, *175*, 239–252.
(11) Regalbuto, J. R.; Navada, A.; Shadid, S.; Bricker, M. L.; Chen, Q. *J. Catal.* **1999**, *184*, 335–348.
(12) Schreier, M.; Regalbuto, J. R. *J. Catal.* **2004**, *225*, 190–202.
(13) Jiao, L.; Regalbuto, J. R. *J. Catal.* **2008**, *260*, 329–341.
(14) D'Souza, L.; Regalbuto, J. R. *J. Catal.* **2007**, *248*, 165–174.
(15) Hao, X.; Barnes, S.; Regalbuto, J. R. *J. Catal.* **2011**, *279*, 48–65.
(16) Pasupong, M. Master's Thesis, University of Illinois at Chicago, Chicago, Illinois, 2011.
(17) Goto, M.; Kasahara, A. *Vacuum* **2006**, *80*, 740–743.
(18) Hwang, C.; Yeh, C. *J. Mol. Catal. A: Chem* **1996**, *112*, 295–302.
(19) Noh, J. S.; Schwarz, J. A. *J. Colloid Interface Sci.* **1990**, *139*, 139–148.
(20) Regalbuto, J. R. *Surface and Nanomolecular Catalysis*; Richards, R., Ed.; Taylor & Francis/CRC Press: Boca Raton, FL, 2006; Chapter 6, p 161.
(21) Regalbuto, J. R. *Catalyst Preparation: Science and Engineering*; Regalbuto, J. R., Ed.; Taylor & Francis/CRC Press: Boca Raton, FL, 2007; Chapter 13, p 297.
(22) Regalbuto, J. R. *Synthesis of Solid Catalysts*; de Jong, K. P., Ed.; Wiley-VCH Verlag: Weinheim, Germany, 2009; Chapter 3, p 33.